LWT - Food Science and Technology 83 (2017) 132–140

Contents lists available at ScienceDirect

LWT - Food Science and Technology

journal homepage: www.elsevier.com/locate/lwt

Development, characterization, and validation of chitosan adsorbed cellulose nanofiber (CNF) films as water resistant and antibacterial food contact packaging

Zilong Deng, Jooyeoun Jung, Yanyun Zhao*

Department of Food Science & Technology, Oregon State University, Corvallis, OR 97331-6602, USA

ARTICLE INFO

Article history:
Received 14 December 2016
Received in revised form
29 March 2017
Accepted 11 May 2017
Available online 13 May 2017

Keywords:
Cellulose nanofiber
Chitosan
Food contact packaging
Water resistance
Antibacterial activity

ABSTRACT

Compatibility of CNF with three polysaccharides having different surface charges and backbones (chitosan, methyl cellulose, and carboxymethyl cellulose) was investigated. Chitosan (CH) incorporation reduced water absorption (WA) of CNF films ($P < 0.05$). CH molecular weight (Mw) (68, 181, 287 kDa) and amount (10 and 20 g/100 g CNF in dry basis) impacted moisture barrier, mechanical, antibacterial, thermal, and structural properties of CNF films. Regardless of Mw, CH incorporation (20 g/100 g CNF) decreased ($P < 0.05$) WA of CNF films, and high Mw (287 kDa) CH (20 g/100 g CNF) incorporation resulted in lower film water solubility while increasing film water vapor permeability compared with low Mw CH (68 kDa) incorporation ($P < 0.05$). CNF film with low Mw CH (20 g/100 g CNF) exhibited antibacterial activity against *L. innocua* and *E. coli*. Interaction mechanisms between CH and CNF were investigated through thermal, structural, and morphology analyses using DSC, FTIR, and SEM, respectively. CNF films with low or high Mw CH incorporation (20 g/100 g CNF) were further validated as surface contact films for fresh beef patties, showing effectiveness to prevent moisture transfer between the layered patties. This study demonstrated the potential of using CNF-CH composite films as water resistant and antibacterial packaging for foods with high moisture surfaces.

1. Introduction

Cellulose nanofiber (CNF) forms films with superior mechanical and gas barrier properties because of its nano-sized dimension, high aspect ratio, surface area, and flexibility (Azeredo, 2009; H.P.S. et al., 2016). However, due to the hydrophilic surface property of CNF, those functional properties of the CNF films may be suppressed by direct moisture contact and/or exposure to high relative humidity (RH) environment (Liu, Walther, Ikkala, Belova, & Berglund, 2011; McHugh, Avena-Bustillos, & Krochta, 1993), thus limiting their application for packaging food products with wet surface, high moisture content, and/or stored at high RH environment. Incorporation of inorganic fillers (i.e. silver), chemical modification (i.e. plasma polymerization or derivatives), and adsorption of other film matrix materials (i.e. xyloglucan or guar gum) have been studied to enhance the water-resistance of CNF films (Eronen, Junka, Laine, & Österberg, 2011; Hernández-Hernández, Neira-Velázquez, Ramos-de, Ponce, & Weinkauf, 2010; Lavoine, Desloges, & Bras, 2014). Among these methods, the adsorption of polymeric materials onto CNF surface avoids the use of strong or harmful chemicals, and is simple, safe and efficient, hence was investigated in this study to develop water resistant packaging films for food with wet and adhesive surfaces.

Polysaccharides are classified based on their surface charges and backbones. Both carboxymethyl cellulose (CMC) and methyl cellulose (MC) are composed of glucose monomers, but contain negatively-charged carboxymethyl (-CH_2COOH) and non-charged relatively hydrophobic methoxyl (-OCH_3) functional groups, respectively. Chitosan (CH) is composed of β-(1–4)-linked D-glucosamine and *N*-acetyl-D-glucosamine with positively-charged amino (-NH_2) groups in acidic solution. The chemical interactions (e.g. hydrogen bonds or electrostatic interactions) and/or physical interactions (e.g. adsorption) of these polysaccharides onto CNF surface vary depending on their functional groups, surface charges, molecular weights (Mw), concentrations, and conformation (Lin & Dufresne, 2014). This study thus selected three types of polysaccharides (CH, MC, and CMC) for understanding their affinities onto CNF surface with different surface charges and backbones and

* Corresponding author.
E-mail address: yanyun.zhao@oregonstate.edu (Y. Zhao).

http://dx.doi.org/10.1016/j.lwt.2017.05.013
0023-6438/

possible impact on the film water-resistant property.

Our previous studies proved that the abundance and availability of the functional amino groups and spatial entanglement of CH vary depending on molecular weight (Mw) of CH (Chen & Zhao, 2012; Jung & Zhao, 2012, 2013). Hence, CH incorporation at different Mw and concentrations into CNF film was tested in this study based on the hypothesis that the affinity of CH with CNF depends on Mw and concentration of CH due to different abundance and availability of the functional amino groups, spatial entanglement and crystallinity of CH, which in turn could impact the physicochemical, mechanical, and antibacterial properties of CNF films. The derived CNF-based films were expected to have sufficient water-resistant and antibacterial properties that can be applied as food contact packaging film to interleave food products with high moist (e.g. meat pieces or patties) surface, thus preventing moisture transfer between layered products.

Therefore, the objectives of this study were to first identify the mostly compatible polysaccharide with CNF to develop water-resistant CNF films and then to validate their applications for contacting food items with wet surfaces and stored under high RH refrigerated temperature. The former objective was achieved through combined two experimental designs: (1) Taguchi design to select the mostly compatible polysaccharide (CMC, MC, or CH) with CNF and (2) completely randomized two factorial design to investigate the influences of Mw and concentration of CH on the properties of CNF films. The derived films were evaluated in physicochemical (color, thickness, haze), water-resistant (water absorption, water solubility, water vapor permeability), mechanical (tensile strength, elongation at break), thermal (differential scanning calorimetry (DSC)), structural (Fourier transform infrared spectroscopy (FT-IR)), and morphological (scanning electron microscopy (SEM)) properties, as well as antibacterial activity against *Listeria innocua* (*L. innocua*) and *Escherichia coli* (*E. coli*). The latter objective was accomplished by applying CNF films with the best performance based upon the first part of studies to layered beef patties as the separation sheets, and evaluating water absorption of films after 1-week refrigerated storage. This study was thus anticipated to provide new insights on the strategies of incorporating functional polysaccharides into CNF for enhancing water resistance and antibacterial activity of CNF films to meet the critical needs of biodegradable antibacterial packaging films and for understanding the mechanisms of improved performance of CNF film based on Mw and concentration of incorporated CH.

2. Materials and methods

2.1. Materials

A CNF slurry (2.95 g/100 g wet basis) was obtained from the Process Development Center of the University of Maine (ME, USA). CNF was extracted from northern bleached softwood kraft pulp by using the Masuko MKZB15-50J super mass collider creating a high shear zone, thus liberating nanofibers present in natural lignocellulosic fibers with dimensions of 20–50 nm in width and up to several hundred microns in length (The Process Development Center, University of Maine, 2016). CMC (400–800 cPs), MC (400 cPs), and CH (97% degree of deacetylation, 287 kDa Mw) were purchased from Alfa Aesar (MA, USA), Sigma Chemical (MO, USA), and Premix (Iceland), respectively. Glycerol was acquired from Fisher Scientific (NJ, USA). Tween 80 and Span 80 were obtained from Amresco (OH, USA). Cellulase was gained from *Aspergillus niger* (TCI America, OR, USA). Ground beef (80% lean and 20% fat) was purchased from a local market on the day that experiment was conducted.

2.2. Chitosan depolymerization

CH was depolymerized to different Mw levels (high: 287 ± 43 kDa, med: 181 ± 18 kDa, and low: 68 ± 2 kDa) through enzymatic hydrolysis using the method from our previous study (Jung & Zhao, 2013). Briefly, high Mw CH (287 kDa) (1 g/100 g) was dissolved in acetic acid (1 g/100 mL distilled water) and adjusted to pH 5 using 10 g/100 mL NaOH. Cellulase (10 g/100 g CH in dry basis) was added to prepared chitosan solutions, and reacted at 50 °C for 5 min or 1.5 h to obtain med or low Mw CH, respectively. The hydrolyzates were boiled for 10 min to inactivate cellulase, and centrifuged at 8500×*g* for 30 min to remove denatured enzyme. Supernatant was then adjusted to pH 9 by NaOH (10 g/100 g in distilled water), and the precipitated portion was washed and collected by centrifugation at 8500×*g* for 30 min. Collected samples were dried at a 40 °C oven overnight. The viscosity-average Mw of CH (0.01 g/100 g 0.1 M CH_3COOH and 0.2 M NaCl) was measured by the Ubbelohde dilution viscometer (Cannon Instrument Co., PA, USA) with a capillary size of 0.58 nm. The intrinsic viscosity was determined by the intercept between the Huggins (reduced viscosity) and Kraemer (relative viscosity) plots. The viscosity-average Mw of CH was calculated using Mark–Houwink–Sakurada (MHS) equation: $[\eta] = K (M_w)^a$, where $K = 1.81 \times 10^{-3}$ mL g^{-1}, a = 0.93, and $[\eta]$ represented the intrinsic viscosity (Jung & Zhao, 2013).

2.3. Preparation of CNF-based films

2.3.1. Development of film formulations

Film formulations were developed using two consecutive experimental designs, Taguchi design (the first part of study) and a completely randomized two factorial design (the second part of study). For Taguchi design (Table 1), CNF (0.75 g/100 g distilled water) and glycerol (10 g/100 g CNF in dry basis) were formulated with different types (CMC, MC, and CH) and concentrations (0, 15, and 30 g/100 g CNF in dry basis) of polysaccharides, avocado oil (0, 15, and 30 g/100 g CNF in dry basis), and surfactant mixture (1:1 of Tween and Span 80, 0, 20, and 40 g/100 CNF in dry basis). Mw of CH used for this part of the study was 287 kDa. Avocado oil was chosen to increase the hydrophobicity of the films, and surfactant was selected to improve the incorporation of hydrophobic compound and decrease the surface tension of the derived films. For a completely randomized two factorial design (Table 2), CNF (0.5 g/100 g distilled water) for creating thinner film and glycerol (10 g/100 g CNF in dry basis) were used along with the addition of the mostly compatible polysaccharide identified from the Taguchi design. In this study, CH was identified as the mostly effective polysaccharide, and different Mw (68, 181, and 287 kDa) and concentrations (10 and 20 g/100 g CNF in dry basis) of CH were incorporated into CNF film formulations. For each concentration of CH, prepared CH solution (3 g/100 mL acetic acid (1 g/100 g distilled water)) was diluted 60 and 30 times, respectively. In this case, the concentration of acetic acid was <0.05 g/100 g for both concentrations of CH. It was previously reported that antibacterial activity of acetic acid starts at 0.166 g/100 mL (Fraise, Wilkinson, Bradley, Oppenheim, & Moiemen, 2013). Hence, the influence of acetate on antibacterial activity of films was negligible in this study.

2.3.2. Preparation of films

Prepared film formulations were homogenized (Polytron PT10-35, Luzernerstrasse, Switzerland) for 5 min, and degassed using a self-build water flow vacuum system (Chen & Zhao, 2012). A 60 mL of formulation was uniformly cast onto 150 mm diameter polystyrene petri dish (Falcon, PA, USA), and dried at room conditions (20 ± 2 °C and 30± 2% RH) for 2 days. Dried films were then conditioned in a self-assembled chamber (Versa, PA, USA) at 25 °C

Table 1
Effects of different polysaccharides (methylcellulose, chitosan, and carboxymethyl cellulose) on water-barrier properties (water vapor permeability (WVP), water absorption ability (WA), and water solubility (WS)) of cellulose nanofiber (CNF)-based films by comparing three respective Taguchi analyses.

Factors and levels*				Methylcellulose (MC)**			Chitosan (CH)**			Carboxymethyl cellulose (CMC)**		
No.	A	B	C	WVP (g mm/m^2 d Pa)	WA (%)	WS (%)	WVP (g mm/m^2 d Pa)	WA (%)	WS (%)	WVP (g mm/m2 d Pa)	WA (%)	WS (%)
1	1	1	1	0.029	435.8	26.56	0.029	392.6	25.20	0.034	354.8	21.69
2	1	2	2	0.035	673.2	32.43	0.030	607.5	30.72	0.040	482.6	18.57
3	1	3	3	0.036	648.5	26.53	0.037	551.6	27.52	0.045	623.3	24.59
4	2	1	2	0.028	540.7	22.70	0.034	172.8	21.86	0.037	ND***	ND
5	2	2	3	0.035	711.9	26.56	0.040	166.8	17.96	0.042	ND	ND
6	2	3	1	0.035	674.7	21.13	0.044	163.4	21.72	0.038	ND	ND
7	3	1	3	0.045	1129.4	27.59	0.044	157.6	26.34	0.041	ND	ND
8	3	2	1	0.036	988.4	36.23	0.045	153.7	22.79	0.038	ND	ND
9	3	3	2	0.038	899.8	30.17	0.045	170.6	23.10	0.043	ND	ND
Factor		Level		Mean values of each factor at each level								
A		A1		0.033 ± 0.004^{a+}	586 ± 131^a	28.5 ± 3.4^{ab}	0.032 ± 0.005^a	517 ± 112^a	27.8 ± 2.8^a	0.040 ± 0.005^a	NA	NA
		A2		0.033 ± 0.004^a	642 ± 90^a	23.5 ± 2.8^a	0.039 ± 0.005^{ab}	168±5^b	20.5 ± 2.2^b	0.039 ± 0.003^a	NA	NA
		A3		0.040 ± 0.005^a	1006 ± 116^b	31.3 ± 4.4^b	0.045 ± 0.001^b	161±9^b	24.1 ± 2.0^{ab}	0.040 ± 0.002^a	NA	NA
		RA^{++}		0.007	420	7.9	0.013	357	7.3	0.002	NA	NA
B		B1		0.034 ± 0.009^a	702 ± 374^a	25.6 ± 2.6^a	0.036 ± 0.008^a	241 ± 132^a	24.5 ± 2.3^a	0.037 ± 0.003^a	NA	NA
		B2		0.035 ± 0.001^a	791 ± 172^a	31.7 ± 4.9^a	0.038 ± 0.008^a	309 ± 258^a	23.8 ± 6.4^a	0.040 ± 0.002^a	NA	NA
		B3		0.036 ± 0.001^a	741 ± 138^a	25.9 ± 4.6^a	0.042 ± 0.004^a	295 ± 222^a	24.1 ± 3.0^a	0.042 ± 0.004^a	NA	NA
		RB^{++}		0.002	89	6.1	0.006	68	0.6	0.005	NA	NA
C		C1		0.033 ± 0.004^a	700 ± 277^a	28.0 ± 7.7^a	0.039 ± 0.009 ^{a}	237 ± 135^a	23.2 ± 1.8^a	0.037 ± 0.002^a	NA	NA
		C2		0.034 ± 0.005^a	705 ± 182^a	28.4 ± 5.1^a	0.037 ± 0.008^a	317 ± 252^a	25.2 ± 4.8^a	0.040 ± 0.003^{ab}	NA	NA
		C3		0.039 ± 0.005^a	830 ± 261^a	26.9 ± 0.6^a	0.040 ± 0.004^a	292 ± 225^a	23.9 ± 5.2^a	0.043 ± 0.002^b	NA	NA
		RC^{++}		0.005	130	1.5	0.004	80	2.0	0.006	NA	NA
Rank^{+++}				A > C > B	A > C > B	A > B > C	A > B > C	A > C > B	A > C > B	C > A > B	NA	NA

* A, B and C represented experimental factors, including concentration of polysaccharide (A_1: 0; A_2: 15%; A_3: 30%, w/w CNF dry base), avocado oil (B_1: 0; B_2: 15%; B_3: 30%, w/w CNF dry base), and surfactant mixture (C_1: 0; C_2: 20%; C_3: 40%, w/w CNF dry base) at a 1:1 ratio of Tween 80 and Span 80, respectively.
** Films were prepared by incorporating 0.75% (w/w water in wet base) CNF and 10% (w/w CNF in dry base) glycerol.
*** ND: Non-detected due to high film solubility; NA: Not applicable.
+ Means followed by the same upper letter in a column were not significantly different ($P > 0.05$).
++ RA, RB, and RC were the largest difference between the highest and lowest values within each factor, indicating the most contributing factor on each measurement.
+++ Ranks were based on the order of RA, RB, and RC values.

Table 2
Effects of chitosan concentrations (CHC) and molecular weights (CHM) on physicochemical (color, thickness, and haze), water-resistant (water absorption (WA), and water solubility (WS)), and mechanical properties (tensile strength and elongation at break) of cellulose nanofiber (CNF)-based films.

	Analysis of variance (ANOVA) results (*P*-value)*						
	ΔE**	Thickness (mm)	TS (MPa)*	WA (%)*	WS (%)*	EB (%)*	Haze (%)
Main factor							
CHC$^+$	<0.0001	<0.0001	0.0240	0.0331	0.6633	0.8312	0.0588
CHM$^+$	0.0003	0.5884	0.8570	0.9261	0.0278	0.5938	0.0810
Interaction factor							
CHC x CHM	0.8251	0.9343	0.8069	0.1281	0.0728	0.9415	0.7315
Levels	*Post hoc* multiple comparison tests^{++}						
	ΔE		Thickness (mm)	TS (MPa)	WA (%)	WS (%)	
	CHC	CHM	CHC	CHC	CHC	CHM	
1	0.62 ± 0.13^a	0.82 ± 0.49^a	0.027 ± 0.000^a	29.5 ± 0.9^a	94.4 ± 10.4^a	31.3 ± 3.3^a	
2	1.33 ± 0.14^b	1.04 ± 0.50^b	0.031 ± 0.001^b	24.9 ± 1.0^b	77.2 ± 9.2^b	28.3 ± 1.7^{ab}	
3		1.07 ± 0.53^b				21.5 ± 7.5^b	

* There was no significant effect of main factor and their interactions when *P*-value was higher than 0.5.
**ΔE, TS, WA, WS, and EB represented the color difference from CNF only film, tensile strength, water absorption ability, water solubility, and elongation at break of CNF films incorporating with different Mw and concentration of chitosan, respectively.
+ Two levels for CHC: 10% and 20% w/w CNF in dry base and three levels for CHM: 68, 181 and 287 kDa.
++ *Post hoc* multiple comparison tests were selectively reported for results showing the significant effect of applied factors in ANOVA result.
All films were prepared by incorporating 0.5% (w/w water in wet base) CNF and 10% (w/w CNF in dry base) glycerol.

and 50% RH for 2 days before all measurements (Chen & Zhao, 2012).

2.4. Evaluation of film properties

2.4.1. Transmission haze and color difference (ΔE)

The transmission haze of the films was measured using a ColorQuest spectrophotometer (HunterLab, VA, USA). Film specimens were placed in front of the sensor and all extraneous light was eliminated before reading. Results were reported in percentage of haze. Color difference (ΔE) of the films was measured using a LabScan XE colorimeter (HunterLab, VA, USA) that was calibrated with a standard white plate ($L^* = 93.87$; $a^* = -0.92$; $b^* = 0.14$). ΔE was calculated as $\Delta E^* = \sqrt{(L^* - L_0^*)^2 + (a^* - a_0^*)^2 + (b^* - b_0^*)^2}$, where L_0^*, a_0^*, and b_0^* represented the color values of 0.5% CNF and

10% glycerol film, and L*, a* and b* referred to the color values of CNF-based films incorporating other materials. Measurements were conducted in triplicates, and mean values were reported.

2.4.2. Mechanical property

Film thickness was measured using a micrometer (NR 293-776-30, Mytutoyo Manufacturing Ltd., Japan) at eight randomly selected locations on each film, and mean value was reported for each replication. Elongation at break (EB, %) and tensile strength (TS, MPa) of the films were determined using a texture analyzer (TA-XT2 Texture Analyzer, Texture Technologies Corp., NY, USA) according to ASTM D882 standard (ASTM, 2001) with some modifications, in which the initial grip separation and crosshead speed were set at 40 mm and 0.4 mm/s, respectively. Film piece (250 × 700 mm) was mounted on a sample grip (TA 96). TS was calculated using maximum load (N) divided by film cross-sectional area (mm^2), and EB (%) was calculated as distance at break divided by the initial length of the specimen and multiplied by 100%. All data were collected in triplicates.

2.4.3. Water absorption ability (WA), water solubility (WS), and contact angle (CA)

Each film specimen (30 × 30 mm) was precisely weighed, and placed in a petri dish with 30 mL of distilled water. After 2 h, samples were placed on paper tissue flatwise to absorb water from the film surface, and then weighed. WA was measured as the percentage weight gain of the films after suspending in water for 2 h. WS was determined by the percentage weight loss of the films after suspending in water for 2 h and drying at 40 °C for 24 h (Zhong, Li, & Zhao, 2012). Both WA and WS were reported as the mean value of three replications.

Hydrophobicity of the film surfaces was evaluated by measuring the contact angle (CA) of the interface between water and film. A 10 μL of distilled water was dropped from 10 mm height to a horizontal flat film specimen (30 × 30 mm) (Hou, Deem, & Choy, 2012), and CA value was determined using CA goniometer (FTA 32, First Ten Angstroms, Inc., VA, USA). A high CA value represented a high water resistance (hydrophobicity) of the film, and data were reported as the mean value of three replications.

2.4.4. Water vapor permeability (WVP)

A cup method was used to measure WVP of the films according to ASTM Standard E96-87 (ASTM, 2000). Cups and lids used for WVP measurements were preconditioned at 25 °C and 50% RH for 24 h. Each film sample (75 × 75 mm) was sealed by vacuum grease on the top of a Plexiglas test cup (57 × 15 mm) filled with 11 mL of distilled water, and the seal ring was tightly closed by rubber bands. Test cup assemblies were stored in a temperature and humidity control chamber (T10RS 1.5, Hyland Scientific, WA, USA) at 25 °C and 50% RH. Each cup assembly was precisely weighed hourly for up to 6 h. Means values of three replications were reported.

2.4.5. Thermal property

Differential scanning calorimetry (DSC) measurements of each film specimen were performed with DSC Q2000 (TA Instruments, New Castle, DE). Sample (11 ± 0.5 mg) was placed into the hermetic aluminum pan (T131219, TA Instruments, DE, USA) and tested from 0 to 300 °C with a heating rate of 20 °C/min under a nitrogen atmosphere at a flow rate of 50 mL/min during all measurements.

2.4.6. Fourier transform infrared spectroscopy (FTIR)

FTIR spectra of the film was determined by Nexus 470 FTIR (Nicolet iS50 FT-IR, Thermo Scientific, WI, USA) equipped with attenuated total reflection (ATR) using diamond crystal with ZnSe focusing element (Nicolet Smart Golden Gate, Specac Ltd, UK). Film specimen (20 × 20 mm) was placed onto ATR-FTIR and the absorbance between 800 and 4000 cm^{-1} with accumulation of 32 scans was collected at a resolution of 4 cm^{-1}.

2.4.7. Morphology of films

The cross-section morphology of CNF films was investigated using SEM (FEI Quanta 600F, OR, USA). The fractured sample obtained from the mechanical measurements was used for imaging the cross-section morphology. Prepared sample was mounted on aluminum stub with the cross-section oriented up and coated by gold palladium alloy sputter coater (Cressington Scientific Instruments Ltd., UK) to improve the interface conductivity. Digital images were collected at an accelerating voltage of 5 kV with a magnification of 20 μm.

2.4.8. Antibacterial activity

Antibacterial activity of films was evaluated using two methods: 1) optical density measurement for quickly evaluating the number of bacteria in enriched culture broth and 2) total plate count method for confirming the data obtained from the optical density measurement. Two non-pathogenic bacterial strains, Gram-positive strain *L. innocua* (ATCC 51742, American Type Culture Collection, VA, USA) and Gram-negative strain *E. coli* (ATCC 25922, American Type Culture Collection), were cultured on brain heart infusion (BHI) agar (Becton, Dickinson and Co., NJ, USA, VA, USA) and tryptic soy agar (TSA) (Becton, Dickinson and Co., NJ, USA), respectively, and stored under 4 °C during the course of the study. Prior to a given microbiological assay, a single typical colony of two bacteria was inoculated in tubes of appropriate broth, and incubated at 37 °C for 24 h (Lab-Line Orbit shaker bath model 3527, IL, USA) with the approximately enriched culture of 10^7 CFU/mL. Two film specimens (10 × 20 mm) were immersed into test tubes with 10 mL of sterilized BHI and tryptic soy broth (TSB), and then inoculated with 100 μL of *E. coli* and *L. innocua*. For the method of optical density measurement, inoculated test tubes without film treatment were used as a negative control (Ctrln) and tubes with CNF only films were applied as positive control (Ctrl). The optical density at 600 nm (OD_{600}) indicating bacterial growth was measured at 0, 5, 10 and 24 h using the UV–Vis spectrophotometer (UV-1800, UV–Vis Spectrophotometer Shimadzu Corporation, Japan) to quickly evaluate the antibacterial effect of the derived films (Zhang, Jung, & Zhao, 2016). The mean values of three replications were reported for treatments and controls.

For measuring the total plate counts of culture broth (Rhee, Lee, Dougherty, & Kang, 2003; Rhim, Hong, Park, & Ng, 2006), 1 mL of sample was taken from the tested tubes at 24 h and added with 9 mL of sterilized peptone solution (0.1 g/100 g distilled water) for the 10-fold serial dilution. Then, 1 mL of sample was immediately transferred into petri dish (n = 2), and plated for the enumeration. BHI agar and tryptic soy agar (TSA) were used for *L. innocua* and *E. coli* enumeration, respectively. Plates were incubated at 37 °C for 48 h, and the number of colonies was counted and reported as $\log_{10}$ CFU/mL.

2.5. Validation study

To validate the performance of developed CNF-CH films, the films were applied as a separation sheet between multi-layered beef patties with high moist surface. A 90 × 90 mm film was precisely weighed and placed between ground beef patties (~80 mm diameter and ~150 g). Six beef patties were stacked together with total five pieces of CNF films, and tested for three stacks for both control and treatments (n = 3). Samples without further packaging were stored at a 5–7 °C refrigerator. After 1-week refrigerated storage, each individual film was reweighed, and WA of film was

calculated as the percentage of weight gain in comparison with the initial weight of the film. The mean values of three replications were reported for control and treatment samples.

2.6. Experimental design and statistical analysis

Taguchi design has been considered as the simple and systematic method for studying the contribution of factors on the measured parameters and for optimizing the treatment conditions with combined levels of each factor (Jung & Zhao, 2011). With nine trials (L_9), Taguchi design was applied to identify the mostly compatible polysaccharide (MC, CH, and CMC) with CNF based on low film WVP, WA and WS. Results were analyzed to investigate statistical significance via *post hoc* least significant difference (LSD) by SAS program (SAS v 9.2, The SAS Institute, USA) and considered to be significantly different at $P < 0.05$.

A completely randomized two factorial design was then applied to the selected polysaccharide (CH in this study) to investigate the effect of CH molecular weight (CHM) and CH concentration (CHC) and their interactive effect on the film functionalities. PROC GLM was utilized to identify significant differences and interaction among each factor using the SAS program, and *post hoc* LSD was tested as the multiple comparisons. All film measurements were conducted in triplicate and results were considered to be significantly different at $P < 0.05$.

3. Results and discussion

3.1. Selection of the most compatible polysaccharide with CNF through Taguchi design

The most compatible polysaccharide with CNF was identified based on WVP, WA, and WS values of the films obtained from three respective Taguchi designs for each polysaccharide (MC, CH, and CMC) (Table 1). For MC incorporation, MC concentration was the highest contributing factor impacting all WVP, WA, and WS values. Significant increase in WA and WS was observed in MC (30 g/100 g CNF) incorporation, indicating weaker affinity of MC to CNF. This might be because the presence of non-polar, hydrophobic methoxyl functional groups in MC impaired the interactions between MC and the hydrophilic CNF surface (Eronen et al., 2011).

For CH incorporation, CH concentration was also the highest contributing factor impacting all WVP, WA, and WS values (Table 1). Although CH incorporation (30 g/100 g CNF) significantly increased WVP (0.045 g mm/m^2 d Pa) of the CNF films ($P < 0.05$), compared to that of CNF only film (0.032 g mm/m^2 d Pa), WA was significantly ($P < 0.05$) reduced in CH-incorporated CNF films. The CH incorporation at 15 g/100 g CNF decreased WS from 27.8% to 20.5% ($P < 0.05$) of CNF films and also achieved a 3 times of reduction on WA compared with the CNF only film without significant impact on WVP. The reduced WA of CH-incorporated CNF films could be due to the partial elimination of the hydrophilic hydroxyl groups from CNF through physicochemical interactions between CH and CNF (Eronen et al., 2011; Nordgren, Eronen, Österberg, Laine, & Rutland, 2009). CH could be adsorbed and well-interacted with CNF owning to their similar conformation structures, and chemically interacted through the hydrogen bonding and electrostatic interaction between the slightly negative-charged CNF and positively-charged CH as well as increasing crystallinity (Khan et al., 2012). The higher WVP of CNF film with CH incorporation could be due to increased crystallinity of film structure that could reduce moisture diffusion through film matrix (Zhong & Xia, 2008). It was also noticed that the addition of different levels of avocado oil and surfactant in CNF films showed no significant difference and had less contribution compared to CH concentration. It was thus concluded that the incorporation of CH at 15 g/100 g CNF improved the water-resistant properties (WA and WS) of CNF film.

For CMC incorporation, the surfactant was the most contributing factor on WVP of the CNF films. WVP was significantly ($P < 0.05$) higher in films with surfactant at 40 g/100 g CNF (0.043 g mm/m^2 d Pa versus 0.037 g mm/m^2 d Pa in film without the surfactant). WA and WS could not be analyzed since CMC-incorporated CNF films were solubilized while testing these parameters. It was probably because the slightly negative-charged CNF surface was not compatible with the negatively-charged CMC through potential electrostatic repulsions (Hatanaka, Yamamoto, & Kadokawa, 2014; Ma, Burger, Hsiao, & Chu, 2014), thus forming loosen matrix of films. Previous studies consistently indicated that CMC-incorporated CNF films was not as strong as both neutral MC and positively charged CH incorporation (Abe, Iwamoto, & Yano, 2007; Eronen et al., 2011). This study confirmed that among 3 tested polysaccharides (CMC, MC, and CH), CH is mostly compatible with CNF in respect to improving water resistance of CNF film. The most suitable Mw and concentration of CH to be incorporated into CNF for improving moisture barrier, mechanical, antibacterial, thermal, structural, and morphological properties of CNF films were then further identified. In addition, the mechanisms of CH incorporation at different Mw and concentrations for improving the performance of CNF film was studied.

3.2. Characterization of CH-incorporated CNF films

According to the results in ANOVA analysis (Table 2 and Fig. 1b), CHM (CH Mw) reported a significant ($P < 0.05$) impact on color difference (ΔE), WS, and WVP of CNF films, whereas CHC (CH concentration) had the significant effect on color, thickness, TS, WA, and WVP of CNF films. There were significant ($P < 0.05$) interactions between CHM and CHC on WVP. In the following sections, only those factors showing a significant effect on measured quality parameters were reported and discussed.

3.2.1. Color difference (ΔE)

Color difference (ΔE) of med (181 kDa) and high (287 kDa) Mw of CH-incorporated CNF films was significantly ($P < 0.05$) higher than that of low (68 kDa) Mw of CH-incorporated CNF films (Table 2). The color change of low Mw CH was diminished, due to the degradation of carotenoid (i.e. astaxanthin) pigment while reducing Mw (Seo, King, & Prinyawiwatkul, 2007). The CH incorporation (20 g/100 g CNF) induced higher ΔE than that of CH incorporation (10 g/100 g CNF) in the films (Table 2) because more carotenoid pigment appeared in high concentration of CH (Hong & Samuel, 1995). Hence, the color of CNF-CH films were affected by Mw and concentration of incorporated CH.

3.2.2. Mechanical property

CNF film was significantly ($P < 0.05$) thicker with CH incorporation at 20 g/100 g CNF (0.031 mm) than that with CH incorporation at 10 g/100 g CNF (0.027 mm) (Table 2), and CH incorporation at 20 g/100 g CNF decreased TS (24.9 MPa) of the CNF film in comparison with CH incorporation at 10 g/100 g CNF (29.5 MPa) (Table 2). CNF with large surface area and high aspect ratio could enhance its mechanical property through physicochemical interactions with CH (Fernandes et al., 2009, 2010). However, CH incorporation at 20 g/100 g CNF could induce polymer agglomeration (Salehudin, Salleh, Mamat, & Muhamad, 2014), thus impacting the compatibility with CNF. Therefore, the concentration of CH influenced the thickness and TS of CNF films.

3.2.3. Water-resistant property

All CH-incorporated CNF films showed significantly ($P < 0.05$)

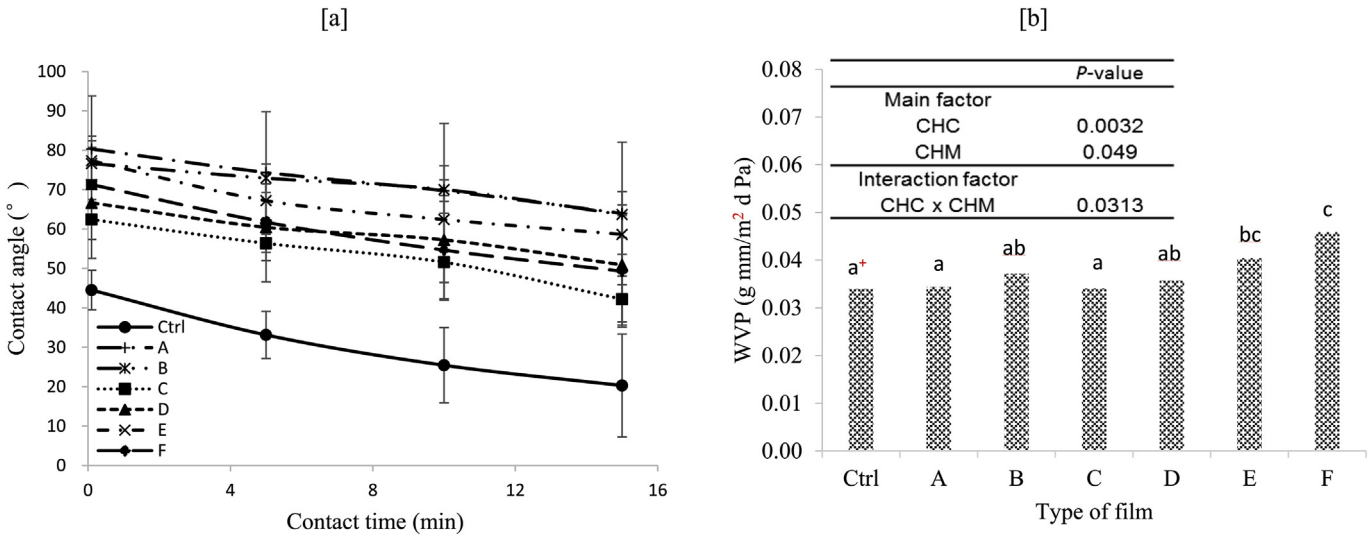

Fig. 1. Effect of chitosan concentration (CHC) and molecular weight (CHM) on contact angle of water on the film surface [a] and water vapor permeability (WVP) [b] of cellulose nanofiber (CNF)-based films; All films were prepared by incorporating 0.5% (w/w water in wet base) CNF and 10% (w/w chitosan in dry base) glycerol; Ctrl = 0% CH, A = 10% CH at 68 kDa, B = 10% CH at 181 kDa, C = 10% CH at 287 kDa, D = 20% CH at 68 kDa, E = 20% CH at 181 kDa and F = 20% CH at 287 kDa, respectively.
[+] Means followed by the same letter were not significantly different ($P > 0.05$).

higher CA in comparison with the CNF only film (Fig. 1a). The adsorption of CH onto CNF led to less available hydroxyl groups of CNF, resulting in less hydrophilic nature of CNF films. For WA and WS, the CH incorporation at 20 g/100 g CNF significantly ($P < 0.05$) reduced WA of the CNF film in comparison with CH incorporation at 10 g/100 g CNF due to the reduced available hydroxyl groups through interactions between CNF and CH. The incorporation of high Mw CH resulted in significantly ($P < 0.05$) lower WS of the film than that of low Mw CH (Table 2), also possibly due to the reduced available hydroxyl groups through interactions between CNF and CH with high Mw. Previous study also reported that CMC, MC, and CH could be irreversibly adsorbed onto the CNF matrix prepared from the kraft pulp (Eronen et al., 2011). These results were consistent with previous studies, showing physicochemical interactions between CNF and CH (Toivonene et al., 2015) and less swelling capacity of CNF films with CH incorporated compared to CNF film (Wu, Farnood, O'Kelly, & Chen, 2014).

CHM, CHC and CHM x CHC showed to have a significant ($P < 0.05$) impact on WVP (Fig. 1b). At 10 g/100 g CHC, there was no significant difference among samples at different Mw; however at 20 g/100 g CHC, low Mw CH incorporation (0.036 g mm/m^2 d Pa) resulted in significantly ($P < 0.05$) lower WVP than that of the high Mw CH (0.06 g mm/m^2 d Pa) due to the decreased moisture diffusion through film matrix. Less moisture diffusion of CNF film incorporated with low Mw CH could be due to free volume decrease, and consequently, moisture diffusion decrease through the films (Cao, Fu, & He, 2007). Thus, it was concluded that low Mw CH formed tightly-packed and water-resistant CH-incorporated CNF films. The CH-incorporated CNF film with improved water-resistance could be applied to food with high moist surface.

3.2.4. Antibacterial property

Antibacterial property of the films was evaluated against both *L. innocua* and *E. coli* by measuring both the optical density of enriched broth at 5, 10 and 24 h and enumerating total bacterial number of broth at 24 h (Fig. 2). For both *L. innocua* and *E. coli*, CNF film incorporated with low Mw CH at 20 g/100 g CNF had the lowest absorbance value after 24 h among all formulations, showing the least bacterial number in the enriched culture broth. This result was also confirmed by total bacterial counts, which was significantly reduced in CNF film with low Mw CH (5.29 $\log_{10}$ CFU/mL) and med Mw CH (5.93 $\log_{10}$ CFU/mL) at 20 g/100 g CNF against *L. innocua*, compared to CNF only film (6.28 $\log_{10}$ CFU/mL). In respect to *E. coli*, bacterial count of broth added with CNF film incorporating low Mw CH at 20 g/100 g CNF was significantly ($P < 0.05$) lower (5.24 log10 CFU/mL) than that with CNF only film (6.68 $\log_{10}$ CFU/mL). These trends were most likely due to the higher availability and releasing of the functional groups (-NH_3^+) in low Mw CH, which was more susceptible to bacteria growth, compared to med and high Mw CH. These results and suggested hypothesis were supported by our previous studies, in which 74 kDa CH had significantly ($P < 0.05$) higher suppression on *E. coli* growth in comparison with 111 kDa and 27 kDa CH (Jung & Zhao, 2013). Hence, the antibacterial activity of CNF films was enhanced by incorporation of low Mw CH at 20 g/100 g CNF. Such films may be utilized as antibacterial packaging for reducing surface contamination of foods.

3.2.5. Structural, thermal, and morphological properties

Fig. 3a shows the FTIR spectrum of CNF-based films. The strong and wide peak in the 3500–3300 cm^{-1} range attributed to the hydrogen-bonded O-H stretching in both CH and CNF, and the overlapping N-H stretching from the primary amine and type II amide in CH appeared in both CNF film and CH-CNF films (Rafieian & Simonsen, 2014), indicating strong interactions between CNF and CH through hydrogen bonds. The spectral bands in the region of 1650 cm^{-1} (amide II carbonyl (–C=O) stretching) were more distinguished in CH-incorporated CNF films than that in CNF film, illustrating the presence of CH in CNF films. Moreover, the spectral band at 1600 cm^{-1} indicating –NH bending of amide I bend attributed from CH was only observed in CH-incorporated CNF films. These results indicated that CH adsorbed onto CNF through hydrogen bonds and/or electrostatic interactions support the forming of improved water-resistant CNF films (Khan et al., 2012).

Fig. 3b illustrates the DSC curves along with the determined glass transition temperature (T_g) of CNF-based films. All compositions exhibited one single broad endothermic peak at slightly different positions, indicating the compatible interactions between

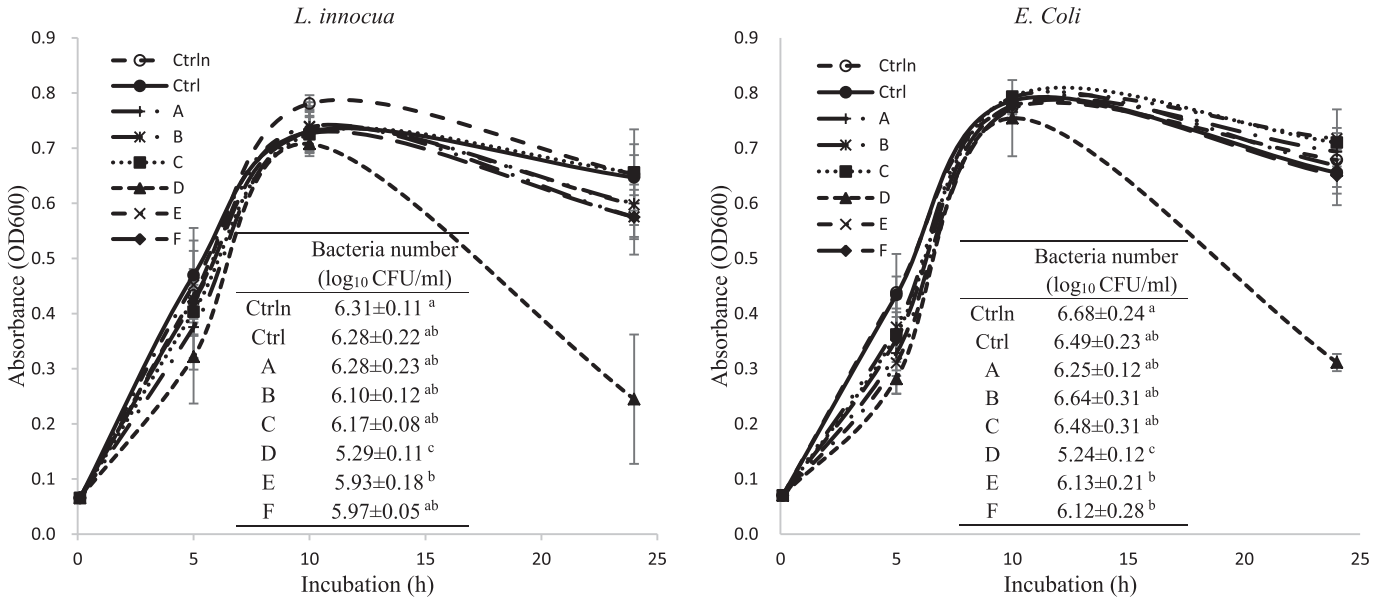

Fig. 2. Inhibition on microbial growth (optical density, OD 600 nm) against *L. innocua* and *E. coli* enrichment broth treated with cellulose nanofiber (CNF)-based films; All films were prepared by incorporating 0.5% (w/w water in wet base) CNF and 10% (w/w chitosan in dry base) glycerol; Ctrl = 0% CH, A = 10% CH at 68 kDa, B = 10% CH at 181 kDa, C = 10% CH at 287 kDa, D = 20% CH at 68 kDa, E = 20% CH at 181 kDa and F = 20% CH at 287 kDa, respectively. Ctrln represented enrichment broth without any film treatment.

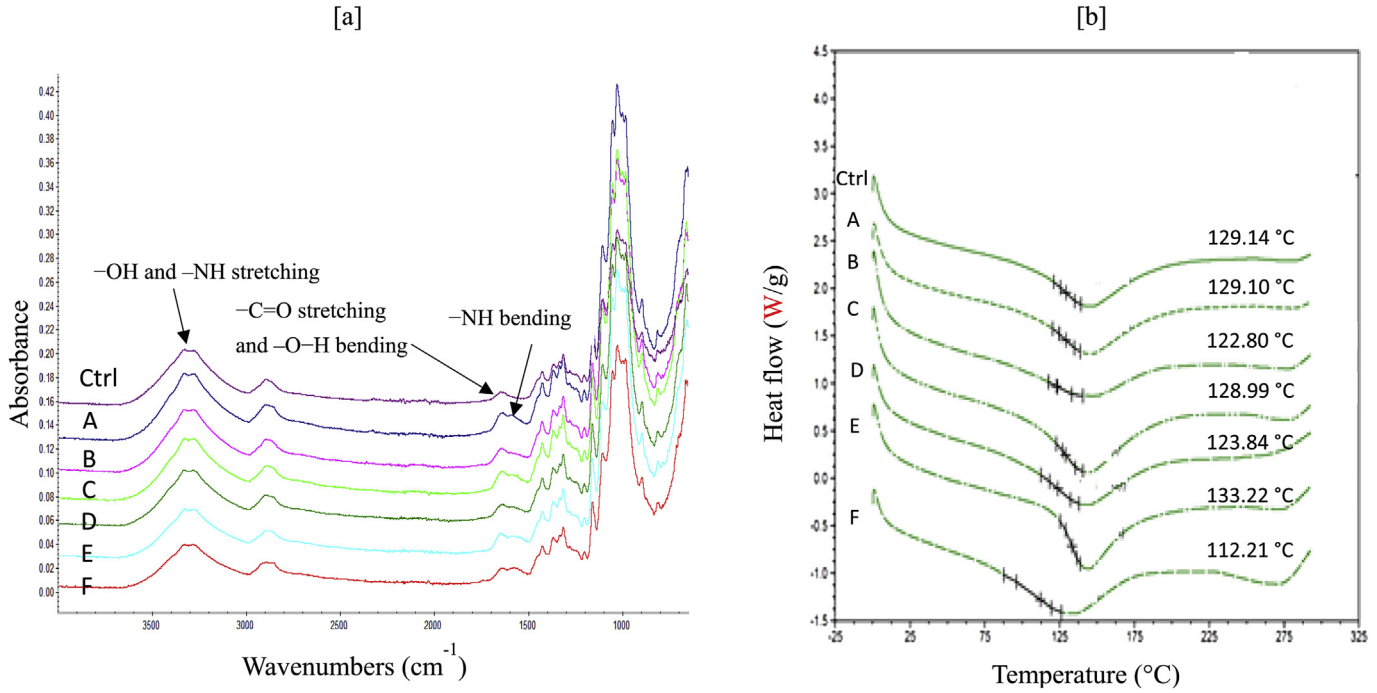

Fig. 3. Fourier transform infrared spectroscopy (FT-IR) [a] and differential scanning calorimetry (DSC) spectrum [b] of cellulose nanofiber (CNF)-based films; All films were prepared by incorporating 0.5% (w/w water in wet base) and 10% (w/w chitosan in dry base) glycerol; Ctrl = 0% CH, A = 10% CH at 68 kDa, B = 10% CH at 181 kDa, C = 10% CH at 287 kDa, D = 20% CH at 68 kDa, E = 20% CH at 181 kDa and F = 20% CH at 287 kDa, respectively; Glass transition temperature (Tg) was determined and reported with DSC spectrum.

the two polymer blends. T_g of CNF film incorporated with med (181 kDa) Mw CH at 20 g/100 g CNF was higher (~133 °C) than that (~129 °C) of CNF only film. The shift of T_g could be the result of improved interactions between the two polymers, which led to a decreased free rotation of amorphous polymeric chains (Azizi Samir, Alloin, Sanchez, & Dufresne, 2004). T_g of CNF film incorporated with high (287 kDa) Mw CH at 20 g/100 g CNF was the lowest (112 °C) among all films. The reduced T_g might be because the incorporation of high Mw CH weakened the interactions (e.g. hydrogen bond) between CNF. However, further studies should be conducted to prove the influence of Mw CH on the polymeric structures of derived films to validate this hypothesis.

Fig. 4 provides the cross-section morphology of CNF films incorporated with low and high Mw CH at 20 g/100 g CNF in comparison with CNF only film. Compared to CNF only (Fig. 4a), CH at low Mw (Fig. 4b) was well-adsorbed into CNF and tightly packed

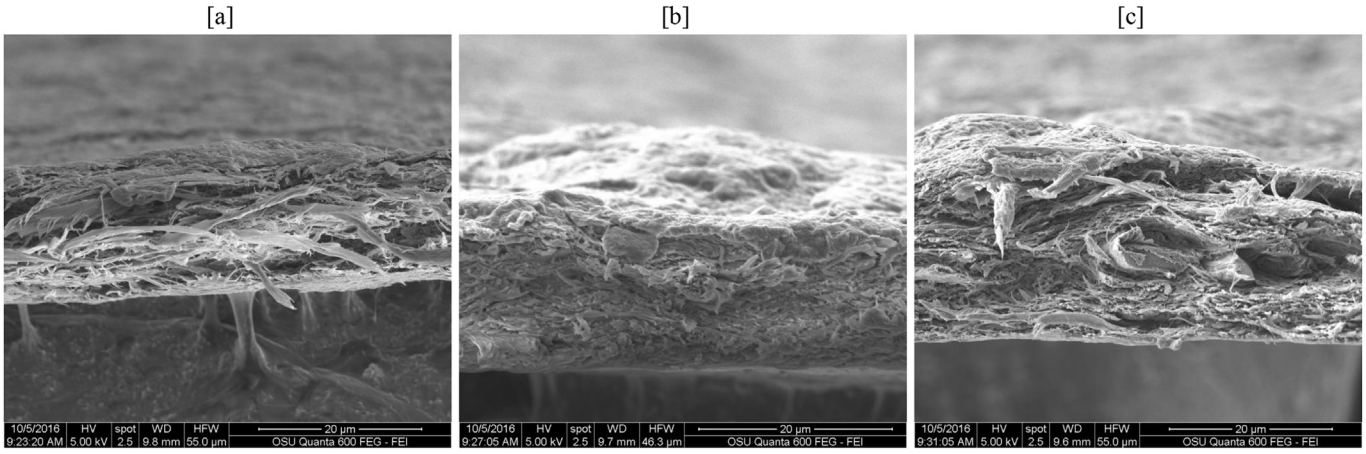

Fig. 4. Cross-section SEM micrographs for CNF only film [a], and low Mw (68 kDa) of chitosan (20% w/w dry base) incorporated CNF film [b], and high Mw (287 kDa) of chitosan (20% w/w dry base) incorporated CNF film [c]; All films were prepared by incorporating 0.5% (w/w water in wet base) CNF and 10% (w/w chitosan in dry base) glycerol. Digital images were collected at an accelerating voltage of 5 kV and with a magnification of 20 µm.

throughout the cross-section matrix possibly due to the strong electrostatic interactions and/or hydrogen bonds between CH and CNF in comparison with CNF only. This result could support the lower WA in CH-incorporated CNF film in comparison with CNF only (Table 1). It was also seen that CNF film with high Mw CH had relatively less packed structures (Fig. 4c), compared to that with low Mw CH (Fig. 4b). This result could be related to the lower WVP in low Mw CH-incorporated CNF films (Fig. 1b) due to less free volumes within film matrix than CNF films with high Mw CH incorporation, allowing less moisture diffusion through film matrix.

3.3. Validation of applying CH-incorporated CNF films for packaging fresh beef patties

Fig. 5 illustrates the appearance of CH-incorporated CNF films as separation sheets placed between beef patties that were stored in a refrigerator (5–7 °C) for 1-week along with measured film WA. CNF only film (Fig. 5a) showed significant color change (pink to red), compared to CH-incorporated CNF films (Fig. 5b and c) because it absorbed more water and blood leaked from the beef patties. Consistently, CH incorporated CNF films had significantly lower liquid absorption (lower WA values) than that of CNF only film (Fig. 5), indicating the enhanced water resistance of CH-incorporated CNF films. These results demonstrated that CH-incorporated CNF films are durable against high moisture condition so that can be potentially applied to high moist surface food as separating sheet to prevent moisture transfer between the layered products. Hence, this study successfully validated that CH-incorporated CNF films can be used as separation sheets between moist surfaces to minimize the moisture transfer between layered food products.

4. Conclusions

This study developed and characterized CNF based films with

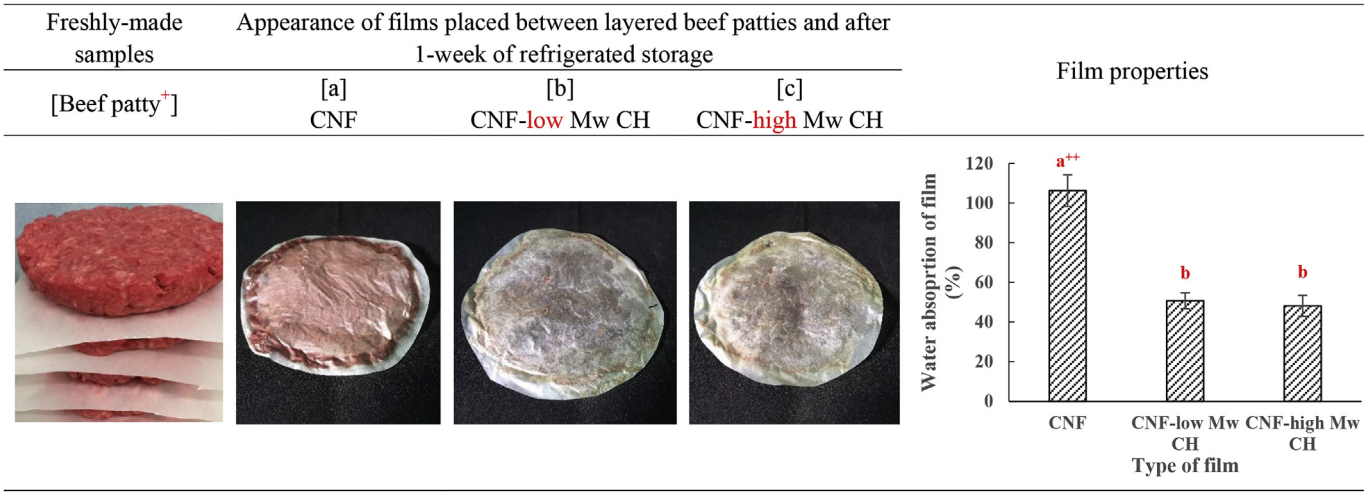

Fig. 5. Demonstration of film applications as separation sheets placed between layered beef patties stored at 5–7 °C for 1 week; [a]: CNF-based film; [b]: low Mw (68 kDa) of chitosan (20% w/w dry base) incorporated CNF-based film; [c]: high Mw (287 kDa) of chitosan (20% w/w dry base) incorporated CNF film; All films were prepared by incorporating 0.5% (w/w water in wet base) CNF and 10% (w/w chitosan in dry base) glycerol.

[+] Ground beef (80% lean and 20% fat) was purchased from a local market on the day when experiment was conducted. A 90 × 90 mm film was precisely weighed and placed between beef patties (~80 mm diameter and ~150 g of each patty).

[++] Means followed by the same letter were not significantly different ($P > 0.05$).

improved water-resistant and antibacterial properties through a simple and safe polysaccharide adsorption method. The type of polysaccharide played an important role in respect to improving the water-resistance of the CNF films. Chitosan incorporation resulted in significant reduction of water absorption, indicating its better compatibility with CNF than methyl cellulose and carboxymethyl cellulose. Mw and concentration of applied chitosan impacted water-resistant and antibacterial properties of chitosan incorporated CNF films. The incorporation of 287 kDa chitosan at 20 g/100 g CNF offered the least water absorption and water solubility of the CNF-CH films, while the incorporation of 68 kDa chitosan at 20 g/100 g CNF provided strong antibacterial property of the CNF films. The developed CNF-CH films as food contact packaging were validated by applying on food products with high moist and adhesive surfaces, and showed their success for reducing moisture loss and adhesion between layered food products. Such films may be utilized as food contact packaging for replacing waxed papers or other synthetic polymers. Future studies are necessary to improve the functional and sealable properties of CNF-CH films by using layer-by-layer assemble and/or other approaches, and also validate their applications in other food products.

References

Abe, K., Iwamoto, S., & Yano, H. (2007). Obtaining cellulose nanofibers with a uniform width of 15 nm from wood. *Biomacromolecules, 8*(10), 3276–3278.

ASTM. (2000). Standard test method for water vapor transmission of materials. E 96–00. In *Annual book of ASTM standards* (pp. 907–914). Philadelphia, Pa.: ASTM Intl..

ASTM. (2001). Standard test method for tensile properties of thin plastic sheeting. D 882–01. In *Annual book of ASTM standards* (pp. 162–170). Philadelphia, Pa.: ASTM Intl..

Azeredo, H. (2009). Nanocomposites for food packaging applications. *Food Research International, 42*(9), 1240–1253.

Azizi Samir, M., Alloin, F., Sanchez, J., & Dufresne, A. (2004). Cellulose nanocrystals reinforced poly(oxyethylene). *Polymer, 45*(12), 4149–4157.

Cao, N., Fu, Y., & He, J. (2007). Mechanical properties of gelatin films cross-linked, respectively, by ferulic acid and tannin acid. *Food Hydrocolloids, 21*(4), 575–584.

Chen, J., & Zhao, Y. (2012). Effect of molecular weight, acid, and plasticizer on the physicochemical and antibacterial properties of β-chitosan based films. *Journal of Food Science, 77*(5), E127–E136.

Eronen, P., Junka, K., Laine, J., & Österberg, M. (2011). Interaction between water soluble polysaccharides and native nanofiber cellulose thin films. *BioResources, 6*(4), 4200–4217.

Fernandes, S., Freire, C., Silvestre, A., Pascoal Neto, C., Gandini, A., Berglund, L., et al. (2010). Transparent chitosan films reinforced with a high content of nanofibrillated cellulose. *Carbohydrate Polymers, 81*(2), 394–401.

Fernandes, S., Freire, C., Silvestre, A., Pascoal Neto, C., Gandini, A., Desbriéres, J., et al. (2009). A study of the distribution of chitosan onto and within a paper sheet using a fluorescent chitosan derivative. *Carbohydrate Polymers, 78*(4), 760–766.

Fraise, A. P., Wilkinson, M. A. C., Bradley, C. R., Oppenheim, N., & Moiemen, N. (2013). The antibacterial activity and stability of acetic acid. *Journal of Hospital Infection, 84*(4), 329–331.

Hatanaka, D., Yamamoto, K., & Kadokawa, J. (2014). Preparation of chitin nanofiber-reinforced carboxymethyl cellulose films. *International Journal of Biological Macromolecules, 69*, 35–38.

Hernández-Hernández, E., Neira-Velázquez, M., Ramos-de, L., Ponce, A., & Weinkauf, D. (2010). Changing the surface characteristics of CNF, from hydrophobic to hydrophilic, via plasma polymerization with acrylic acid. *Journal of Nano Research, 9*, 45–53.

Hong, K., & Samuel, P. (1995). Preparation and characterization of chitin and chitosan—a review. *Journal of Aquatic Food Product Technology, 4*(2), 27–52.

Hou, X., Deem, P., & Choy, K. (2012). Hydrophobicity study of polytetrafluoroethylene nanocomposite films. *Thin Solid Films, 520*(15), 4916–4920.

H.P.S., A., Saurabh, C., A.S., A., Nurul Fazita, M., Syakir, M., Davoudpour, Y., et al. (2016). A review on chitosan-cellulose blends and nanocellulose reinforced chitosan biocomposites: Properties and their applications. *Carbohydrate Polymers, 150*, 216–226.

Jung, J., & Zhao, Y. (2011). Characteristics of deacetylation and depolymerization of β-chitin from jumbo squid (*Dosidicus Gigas*) pens. *Carbohydrate Research, 346*(13), 1876–1884.

Jung, J., & Zhao, Y. (2012). Comparison in antioxidant action between α-chitosan and β-chitosan at a wide range of molecular weight and chitosan concentration. *Bioorganic & Medicinal Chemistry, 20*(9), 2905–2911.

Jung, J., & Zhao, Y. (2013). Impact of the structural differences between α- and β-chitosan on their depolymerizing reaction and antibacterial activity. *Journal of Agricultural and Food Chemistry, 61*(37), 8783–8789.

Khan, A., Khan, R., Salmieri, S., Le Tien, C., Riedl, B., Bouchard, J., et al. (2012). Mechanical and barrier properties of nanocrystalline cellulose reinforced chitosan based nanocomposite films. *Carbohydrate Polymers, 90*(4), 1601–1608.

Lavoine, N., Desloges, I., & Bras, J. (2014). Microfibrillated cellulose coatings as new release systems for active packaging. *Carbohydrate Polymers, 103*, 528–537.

Lin, N., & Dufresne, A. (2014). Nanocellulose in biomedicine: Current status and future prospect. *European Polymer Journal, 59*, 302–325.

Liu, A., Walther, A., Ikkala, O., Belova, L., & Berglund, L. (2011). Clay nanopaper with tough cellulose nanofiber matrix for fire retardancy and gas barrier functions. *Biomacromolecules, 12*(3), 633–641.

Ma, H., Burger, C., Hsiao, B., & Chu, B. (2014). Fabrication and characterization of cellulose nanofiber based thin-film nanofibrous composite membranes. *Journal of Membrane Science, 454*, 272–282.

McHugh, T., Avena-Bustillos, R., & Krochta, J. (1993). Hydrophilic edible films: Modified procedure for water vapor permeability and explanation of thickness effects. *Journal of Food Science, 58*(4), 899–903.

Nordgren, N., Eronen, P., Österberg, M., Laine, J., & Rutland, M. (2009). Mediation of the nanotribological properties of cellulose by chitosan adsorption. *Biomacromolecules, 10*(3), 645–650.

Rafieian, F., & Simonsen, J. (2014). Fabrication and characterization of carboxylated cellulose nanocrystals reinforced glutenin nanocomposite. *Cellulose, 21*(6), 4167–4180.

Rhee, M.-S., Lee, S.-Y., Dougherty, R. H., & Kang, D.-H. (2003). Antimicrobial effects of mustard flour and acetic acid against Escherichia coli O157:H7, Listeria monocytogenes, and Salmonella enterica Serovar Typhimurium. *Applied and Environmental Microbiology, 69*(5), 2959–2963.

Rhim, J.-W., Hong, S.-I., Park, H.-M., & Ng, P. K. W. (2006). Preparation and characterization of chitosan-based nanocomposite films with antimicrobial activity. *Journal of Agricultural and Food Chemistry, 54*(16), 5814–5822.

Salehudin, M., Salleh, E., Mamat, S., & Muhamad, I. (2014). Starch based active packaging film reinforced with empty fruit bunch (EFB) cellulose nanofiber. In *Procedia Chemistry, 9* pp. 23–33). International Conference and Workshop on Chemical Engineering, UNPAR 2013 (ICCE UNPAR 2013).

Seo, S., King, J. m., & Prinyawiwatkul, W. (2007). Simultaneous depolymerization and decolorization of chitosan by ozone treatment. *Journal of Food Science, 72*(9), C522–C526.

The Process Development Center, University of Maine. (2016). *Nanocellulose facility - nanocellulose spec sheets and safety data sheets*. Available from: https://umaine.edu/pdc/facilities-available-for-use/nanocellulose-facility/nanocellulose-spec-sheets-and-safety-data-sheets/.

Toivonene, M. S., Kurki-Suonio, S., Schacher, F. H., Hietala, S., Rojas, O. J., & Ikkala, O. (2015). Water-resistant, transparent hybrid nanopaper by physical cross-linking with chitosan. *Biomacromolecules, 16*(3), 1062–1071.

Wu, T., Farnood, R., O'Kelly, K., & Chen, B. (2014). Mechanical behavior of transparent nanofibrillar cellulose–chitosan nanocomposite films in dry and wet conditions. *Journal of the Mechanical Behavior of Biomedical Materials, 32*, 279–286.

Zhang, H., Jung, J., & Zhao, J. (2016). Preparation, characterization and evaluation of antibacterial activity of catechins and catechins-Zn complex loaded β-chitosan nanoparticles of different particle sizes. *Carbohydrate Polymers, 137*, 82–91.

Zhong, Y., Li, Y., & Zhao, Y. (2012). Physicochemical, microstructural, and antibacterial properties of β-chitosan and Kudzu starch composite films. *Journal of Food Science, 77*(10), E280–E286.

Zhong, Q., & Xia, W. (2008). Physicochemical properties of edible and preservative films from chitosan/cassava starch/gelatin blend plasticized with glycerol. *Food Technology Biotechnology, 46*(3), 262–269.